

# Fluorescence anisotropy of rhodamine 6G using incoherent laser light

Attieh A AL-Ghamdi<sup>a</sup>, Angus J Bain<sup>b</sup>

<sup>a</sup>Institute of Space Research  
King Abdulaziz City for Science and Technology,  
Riyadh, Saudi Arabia e-mail: alghamdi@kacst.edu.sa

<sup>b</sup>Physics Department, University of Essex  
Wivenhoe Park, Colchester, Essex CO4 3SQ, England

## ABSTRACT

A novel method for fluorescence anisotropy using incoherent laser light is presented. The incoherent upconversion technique to measure picosecond molecular motion of rhodamine 6G is investigated experimentally.

**Keywords:** anisotropy, incoherent, fluorescence, upconversion, frequency mixing

## 1. INTRODUCTION

Due to the anisotropy nature of the transition probability the absorption of polarized light by molecules in a liquid creates an initially ordered array of excited states<sup>1</sup>. The subsequent fluorescence from this population will be polarized, the degree of polarization reflecting the anisotropy persisting in the system. The degree of fluorescence polarization (anisotropy) will decrease in time due to molecular rotational arising from Brownian motion in the liquid. Picosecond fluorescence anisotropy measurements have been shown to be sensitive probes of molecular motion and have been used to study a wide range of systems covering simple binary solutions<sup>2</sup> to membranes<sup>3</sup> and liquid crystals<sup>4</sup>. A comprehensive review of fluorescence polarization in condensed matter is given by Burghardt<sup>5</sup>.

Fluorescence anisotropy measurements can be made using upconversion. This was first performed by Beddard and co-workers<sup>6</sup> using synchronously pumped dye laser pulses on a picosecond timescale to initiate and subsequently gate molecular fluorescence in LiIO<sub>2</sub> crystal. By exploiting the polarization sensitivity of sum-frequency generation it is possible to deconvolute population and orientational decays from the gated signal<sup>7</sup>.

Incoherent upconversion using the 38 ps Gaussian noise structure of 532 nm Q-switched Nd:YAG laser pulses could be used to recover nanosecond fluorescence decays despite the presence of an unavoidable and significant background signal<sup>8</sup>. A consideration of the form of upconverted fluorescence signal  $D(\tau)$  as a function of the ratio of the laser coherence to the fluorescence lifetime ( $\tau_{coh}/\tau_f$ ) indicated that accurate signal recovery is made easier as  $\tau_{coh}$  is increased to within an order of magnitude to that of  $\tau_f$ <sup>9</sup>. With the current incoherent upconversion apparatus the resolution of picosecond domain fluorescence transients fall into this category. In this paper the use of incoherent upconversion to measure picosecond fluorescence anisotropy in Rhodamine 6G is investigated.

## 2. COHERENT POLARISED FLUORESCENCE

For conventional upconversion (using Mode-locked laser) with a Gaussian pulsewidth  $\tau_p$  the upconverted parallel and perpendicularly polarized fluorescence intensities following short pulse excitation are given by<sup>10</sup>

$$I_{\parallel}(\tau) = \int_{-\infty}^{\tau} \left( b \cdot \exp - 4 \ln(2) \left( \frac{t'}{\tau_p} \right)^2 \right) \cdot B' \left\{ \exp - (\gamma_f(\tau - t')) \left[ 1 + \frac{2 \langle \alpha_{20}(0) \rangle}{\sqrt{5}} \exp - (\gamma_{or}(\tau - t')) \right] \right\} dt' \quad (1)$$

and

$$I_{\perp}(\tau) = \int_{-\infty}^{\tau} \left[ b \cdot \exp - 4 \ln(2) \left( \frac{t'}{\tau_p} \right)^2 \right] \cdot B' \left\{ \exp - (\gamma_f(\tau - t')) \left[ 1 - \frac{\langle \alpha_{20}(0) \rangle}{\sqrt{5}} \exp - (\gamma_{or}(\tau - t')) \right] \right\} dt' \quad (2)$$

Where  $I_{\parallel}(\tau)$  and  $I_{\perp}(\tau)$  are the parallel and perpendicular fluorescence intensities components with respect to the incident laser polarization,  $B'$  constant of proportionality,  $\langle \alpha_{20}(0) \rangle$  is the initial degree of alignment,  $\gamma_f$  is the excited state fluorescence decay rate,  $\gamma_{or}$  is the reorientational decay rate,  $\tau_p$  is the gaussian laser pulse for mode-locked laser and  $b$  is a scaling factor. These two quantities can be used to construct what is termed the fluorescence anisotropy  $R(t)$  through the relation<sup>11</sup>

$$R(t) = \frac{I_{\parallel}(t) - I_{\perp}(t)}{I_{\parallel}(t) + 2I_{\perp}(t)} \quad (3)$$

Substitution of equation (1) and (2) into (3) yields

$$R(t) = \frac{\langle \alpha_{20}(t) \rangle}{\sqrt{5}} \quad (4)$$

The fluorescence anisotropy is directly proportional to the degree of alignment present in the excited state at time  $t$ . Immediately following excitation  $\langle \alpha_{20}(0) \rangle$  is  $2/\sqrt{5}$  (see equation (4)) and  $R(0)$  is 0.4.

Collisions between excited molecules and their surroundings result in the randomization of this anisotropic distribution which will result in a zero value for  $\langle \alpha_{20} \rangle$  at some time after excitation. In the case of simple isotropic rotational diffusion in which the transition moments are parallel and lie along a molecular symmetry axis  $\langle \alpha_{20}(t) \rangle$  decays exponentially,

$$R(t) = R(0) \exp - \frac{t}{\tau_{or}} \quad (5)$$

where  $\tau_{or}$  is the orientational relaxation time and  $R(0)$  is the initial anisotropy induced by the laser pulse<sup>11</sup>.

By using equations (1) and (2) the calculated fluorescence profiles parallel and perpendicular to the excitation polarization are shown in figures (1.a) with  $\tau_f = 3$  ns and  $\tau_{or} = 250$  ps, and laser pulse width of 38 ps. The corresponding fluorescence anisotropy  $R(t)$  then using equation (3) is shown in figure (1.b).

### 3. INCOHERENT POLARISED FLUORESCENCE

Incoherent fluorescence upconversion can be used in principle to measure fluorescence anisotropies and determine molecular reorientational times<sup>9</sup>. For incoherent upconversion with a continuous wave noiseburst the upconverted fluorescence intensities are given by<sup>9</sup>

$$I_{\parallel}(\tau) = \int_{-\infty}^{\tau} \left[ 1 + b \cdot \exp - \left( \frac{\sqrt{\pi} t'}{\tau_{coh}} \right)^2 \right] \cdot \left\{ \exp - (\gamma_f(\tau - t')) \left[ 1 + 2R(0) \exp - (\gamma_{or}(\tau - t')) \right] \right\} dt' \quad (6)$$

and

$$I_{\perp}(\tau) = \int_{-\infty}^{\tau} \left[ 1 + b \cdot \exp\left(-\left(\frac{\sqrt{\pi}t'}{\tau_{coh}}\right)^2\right) \right] \cdot \left\{ \exp\left(-\gamma_f(\tau-t')\right) \left[ 1 - R(0) \exp\left(-\gamma_{or}(\tau-t')\right) \right] \right\} dt' \quad (7)$$

Where  $b$  is a scaling factor to account for the possibility of a less than 100% correlation between the fluorescence and the gating pulse in the mixing crystal. Setting  $t = t'/\tau_{coh}$   $dt' = \tau_{coh}dt$ . Dividing by  $\tau_f$  and letting  $a = \tau_{coh}/\tau_f$ ,  $d = \tau_{coh}/\tau_{or}$  and  $x = \tau/\tau_{coh}$ , equations (6) and (7) can be written as

$$I_{\parallel}(x) = 1 + 2R(0)\left(1/(1+d/a)\right) + a \cdot b \cdot \exp\left(-x \cdot a\right) \int_{-\infty}^x \exp\left(-(\sqrt{\pi}t)^2\right) \exp(a \cdot t) \cdot dt \quad (8)$$

$$+ 2 \cdot b \cdot R(0) \cdot a \cdot \exp\left(-((x \cdot a) + (x \cdot d))\right) \int_{-\infty}^x \exp\left(-(\sqrt{\pi}t)^2\right) \exp\left((a+d) \cdot t\right) dt$$

and

$$I_{\perp}(x) = 1 - R(0)\left(1/(1+d/a)\right) + a \cdot b \cdot \exp\left(-x \cdot a\right) \int_{-\infty}^x \exp\left(-(\sqrt{\pi}t)^2\right) \exp(a \cdot t) \cdot dt \quad (9)$$

$$- R(0) \cdot a \cdot b \cdot \exp\left(-((x \cdot a) + (x \cdot d))\right) \int_{-\infty}^x \exp\left(-(\sqrt{\pi}t)^2\right) \exp\left((a+d) \cdot t\right) dt$$

Equations (8) and (9) are the fitting functions for  $I_{\parallel}(x)$  and  $I_{\perp}(x)$ .

The form of the upconverted fluorescence signals  $I_{\parallel}(x)$  and  $I_{\perp}(x)$  are shown in figure (2) where a laser coherence time of 38 ps is assumed together with orientational and fluorescence lifetimes of 250 ps and 3 ns respectively. It can be seen that the apparent decays are superimposed on different background signals reflecting the difference in the time averaged fluorescence intensities for parallel and perpendicular emission polarizations.

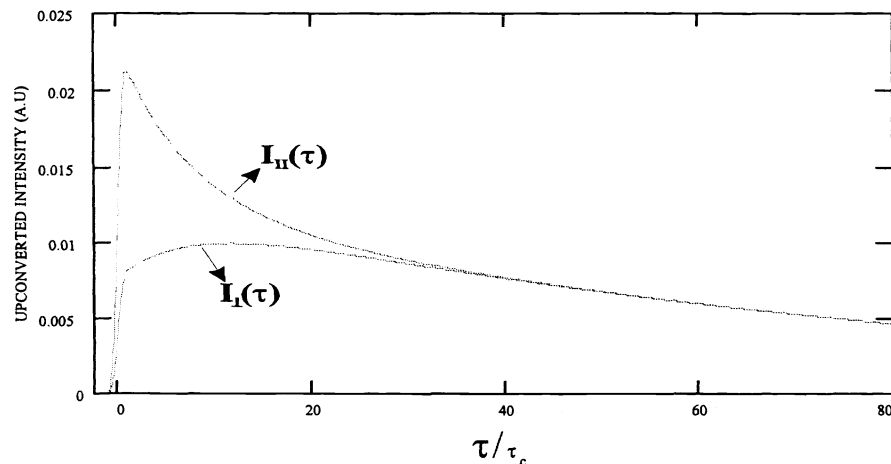


**Figure (1.a).** Calculated upconverted fluorescence profiles for parallel  $I_{\parallel}$  and perpendicular  $I_{\perp}$  pump to probe cases from equations (1) and (2) respectively. The input parameters were;  $\tau_p=38$  ps (pulsed assumed to be Gaussian),  $\tau_f=3$  ns and  $\tau_{or}=250$  ps.

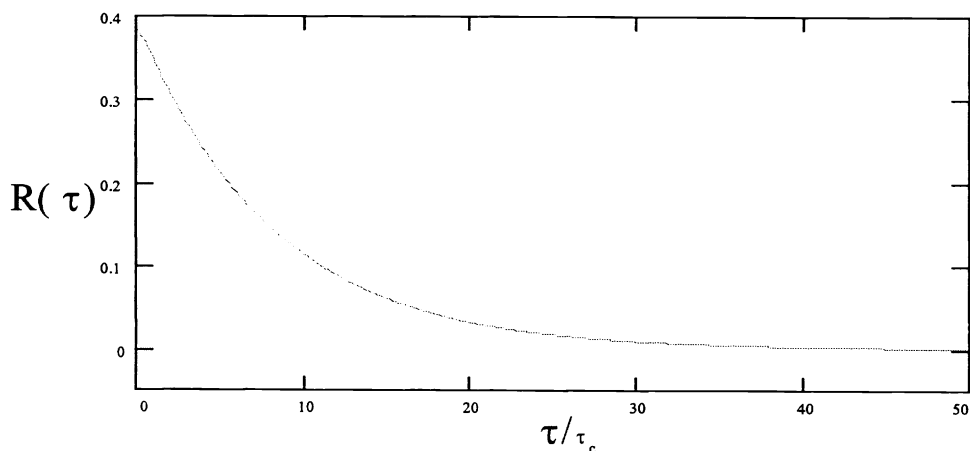


**Figure (1.b)** Calculated fluorescence anisotropy from the  $I_{\parallel}$  and  $I_{\perp}$  decays shown in figure (1.a).

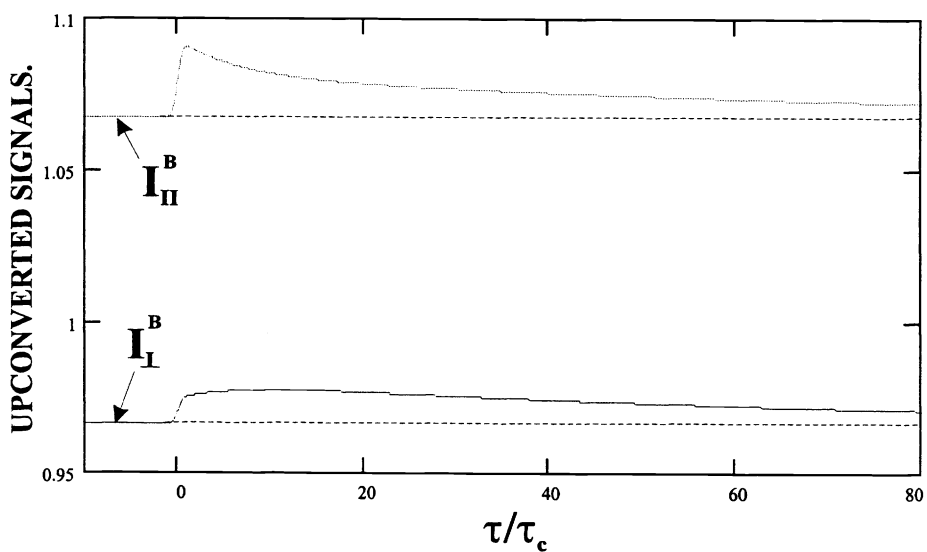


**Figure (2).** Fluorescence profiles calculated parallel  $I_{\parallel}(\tau)$  and perpendicular  $I_{\perp}(\tau)$  to the excitation incoherent laser light respectively with  $\tau_f = 3$  ns and  $\tau_{or} = 250$  ps.

For parallel and perpendicular emission polarizations these are given by

$$I_{\parallel}^B = 1 + 2R(0) \left( \frac{\tau_{or}}{\tau_f + \tau_{or}} \right) \quad (10)$$

$$I_{\perp}^B = 1 - R(0) \left( \frac{\tau_{or}}{\tau_f + \tau_{or}} \right) \quad (11)$$

Construction of the orientational anisotropy decay from the direct combination of  $I_{\parallel}$  and  $I_{\perp}$  data is only possible in principle in the limit where the fluorescence lifetime is long and the fluorescence background becomes unpolarised (see figure (3)). A further complication may arise in practice as the parallel and perpendicular emission polarizations will be affected by any inherent polarization bias in the optics and the upconversion process. Subtraction of the time averaged background signals from both the  $I_{\parallel}(\tau)$  and  $I_{\perp}(\tau)$  curves will yield decays that may be weighted by what is termed the instrumental  $g$ -factor. The  $g$ -factor can be determined in a number of ways one of the most common is to tail match the  $I_{\parallel}(\tau)$  and  $I_{\perp}(\tau)$  decays which should equal at large values of  $\tau$  for isotropic rotational diffusion<sup>1</sup>

$$g = \frac{I_{\parallel}(\tau_{\text{large}})}{I_{\perp}(\tau_{\text{large}})} \quad (12)$$

From these considerations a suitable procedure for the resolution of incoherent fluorescence polarization observables would be the collection of  $I_{\parallel}(\tau)$  and  $I_{\perp}(\tau)$  data with sufficient resolution to allow accurate background subtraction followed by tail matching of the decay curves obtained to determine the  $g$ -factor of the experimental apparatus. The modified  $I_{\parallel}(\tau)$  and  $I_{\perp}(\tau)$  data could then be used to construct the  $R(\tau)$  decay profile for the system. In cases where the data is not of sufficient quality to allow such procedure the orientational decays could still be determined by a two exponential fit to the  $I_{\parallel}(\tau)$  signal which contains the largest  $\langle \alpha_{20}(t) \rangle$  contribution.

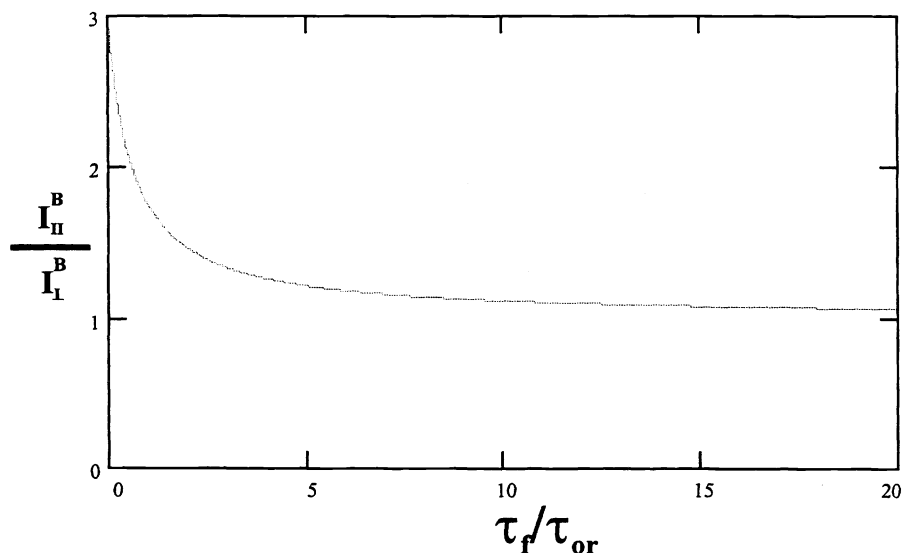


**Figure (3).** A plot of the ratio of the parallel and perpendicularly polarized background upconversion signals as a function of the relative reorientational and fluorescence decay rates. In the limit where  $\gamma_{or}$  is large, The time averaged fluorescence is effectively unpolarised and the two background signals are equal.

#### 4. Experimental Detail

The Nd:YAG oscillator (Spectron SL400) resonator design follows a Sarkies type resonator<sup>12</sup>, which has been extensively investigated by Hanna and coworkers<sup>13</sup>. An intracavity quartz polariser and temperature stabilized KD\*P Pockels cell provide Q-switched pulsed operation through a 3.5% reflecting output coupler giving approximately 140mJ pulses at 1064nm at a repetition rate of 10Hz. The Nd:YAG output is frequency doubled in a heated KD\*P crystal (type 2 phasematching). The residual fundamental is separated by means of a dichroic beamsplitter giving up to 60mJ per pulse at 532nm.

For second harmonic generation autocorrelation, background free autocorrelation measurements (non-collinear SHG technique) were chosen because the constant ratio between the height of the signal to background (2:1) is higher than in the case of a collinear autocorrelation measurement.

The input intensity of 532 nm Nd:YAG pulses to the autocorrelation apparatus (figure 4) was controlled by a high energy Glan-Taylor polariser ( $P_1$ ) and half wave plate ( $\lambda_1$ ) combination. Typical input energies were in the range of 15-20 $\mu$ J. After recollimation with a 2 m focal length lens  $L_1$  the input was split into two horizontally polarised components of equal intensity by means of a half wave plate and beamsplitter cube combination ( $\lambda_2, B_1$ ). A secondary half wave plate and prism polariser combination ( $\lambda_3, P_2$ ) were used for horizontally polarised light. Both beams were subsequently recombined at an angle of 3.8° with 25 cm focal length lenses  $L_2$  and  $L_3$  in a 100  $\mu$ m KD\*P doubling crystal. One beam traverse a fixed optical delay via the retroreflector corner cube  $R_1$ , the other suffered a variable delay via the retroreflector  $R_2$  mounted on a computer controlled translation stage. The two beam SHG signal was spatially filtered from the single beam signal using an iris diaphragm  $i_1$ . The fundamental was removed by means of a UG11 filter ( $F_1$ ) and a uv monochromator (Jobin Yvon model H.10). Recollimation and focusing into the monochromator was achieved by uv 6.5 cm and 15 cm focal length lenses ( $L_4$  and  $L_5$ ). The SHG signal at 266 nm was detected by an (Thorn) EM1 photomultiplier tube (Model RFIB217F) and the resulting signal was averaged by a Boxcar Integrator (Stanford Research System Model 250). The signal was recorded as a function of delay line position (relative path length difference between the two beams). A computer program was written to control the delay line position and allow the collection of data from the boxcar for successive increments in the delay line position.

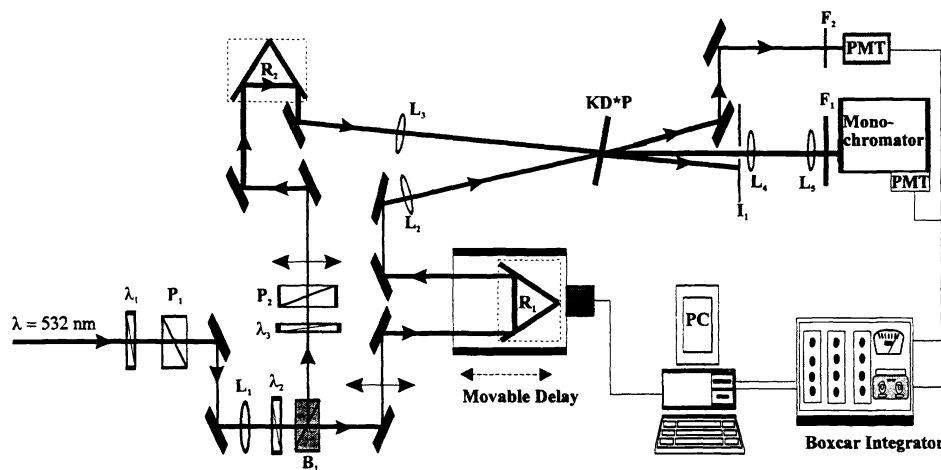


**Figure (4).** Schematic diagram of the autocorrelation using non-collinear second harmonic generation technique.

The frequency-doubled Q-switched nanosecond laser used in this work has a coherence time,  $\tau_{coh}$ , that is short in comparison to the 10 nanosecond pulse envelope. This coherence time  $\tau_{coh}$  is obtained from a fit to the equation  $1 + \exp\left(-\sqrt{\pi}t/\tau_{coh}\right)$ .

The diagram in figure (5) represents a part of the incoherent fluorescence upconversion experiment (the area surrounded by the rectangular dashed line of figure 4). Our sample Rhodamine 6G is an organic dye operating in the visible with high efficiency and strong absorption band at 532nm. When excited by 532nm, it display intense broadband fluorescence spectra. For upconversion measurements on Rhodamine 6G a quartz flow cell (Helma) containing a c.a.  $10^{-3}$  M solution of the dye was

inserted in one arm with the gating 532 nm pulses undergoing a variable optical delay in the other arm (see figure 5). The pump pulses are focused into the flow cell using a 10 cm lens ( $L_3$ ) the fluorescence is collected and collimated by a 2.5 cm achromatic lens and sent through a red pass filter (Schott OG 750) to remove any remaining pump light before focusing into the KD\*P with a 3.5 cm achromatic lens. The gating pulse is focused into the KD\*P with a 25 cm lens ( $L_2$ ). Both beams are non-collinearly overlapped at a small angle (c.a.  $3.8^\circ$ ) and are spatially filtered after passing through KD\*P with an iris diaphragm. Insertion of a Glan-Taylor polariser (Leysop Ltd) between the two achromatic collection lenses in the upconversion apparatus (see figure 5) allows the selection of parallel and perpendicularly polarised fluorescence emission (defined relative to the horizontal pump polarization). The upconverted signal for a given pump-gate separation was collimated and focused onto the 200  $\mu\text{m}$  slits of a Monochromator (Jobin Yvon HR.10) prior to detection by a UV sensitive Photomultiplier (EMI RB 217F). For accurate lifetime measurements it is also important to normalize the upconverted signal to account for shot to shot fluctuations the pump and gate pulses. The upconverted signal should show a quadratic dependence in the 532 nm pulse intensity. For this reason a convenient normalization signal is provided by a frequency doubled portion of the 532 nm Nd:YAG output in an additional KD\*P crystal giving a 266 nm signal which is filtered from the fundamental by a uv pass filter (Schott UG.11) before detection with a photomultiplier (model EMI RB 217F) as in figure 4.

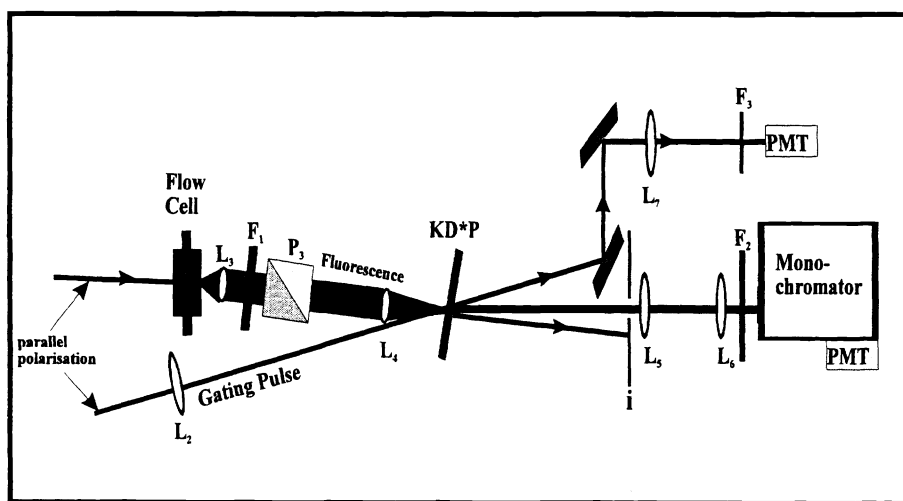


**Figure (5).** The diagram represents a part of the incoherent fluorescence upconversion experiment. A polariser ( $P_3$ ) was inserted between the filter ( $F_1$ ) and lens ( $L_4$ ). The fluorescence can be collected with polarization parallel and perpendicular to the polarization of the exciting light for Rhodamine 6G solution as indicated in the graph.

## 5. RESULTS AND DISCUSSION

Figure (6) shows a typical normalized SHG autocorrelation trace of the frequency-doubled Nd:YAG laser. The normalized data is comprised of one hundred points and is the result of 25 scans, and a 10 shot time-average setting on the Boxcar Integrator. This trace, having an autocorrelation coefficient of  $\approx 2$ , is characteristic of a Gaussian statistical light field. In addition figure (7) shows the result of extending this SHG autocorrelation trace, revealing a broad background with marked curvature. This background originates from the autocorrelation of the 10 ns incoherent pulse envelope<sup>9</sup>. From the analysis of the phase matching in KD\*P as in reference [9] it was concluded that in upconversion experiment fully phase matched type I and type II nonlinear SFG was not simultaneously possible. However given the short (100  $\mu\text{m}$ ) path length of the KD\*P crystal the phase matching constraints appear to be considerably relaxed as both input polarizations were found to give upconversion signals of a comparable magnitude.

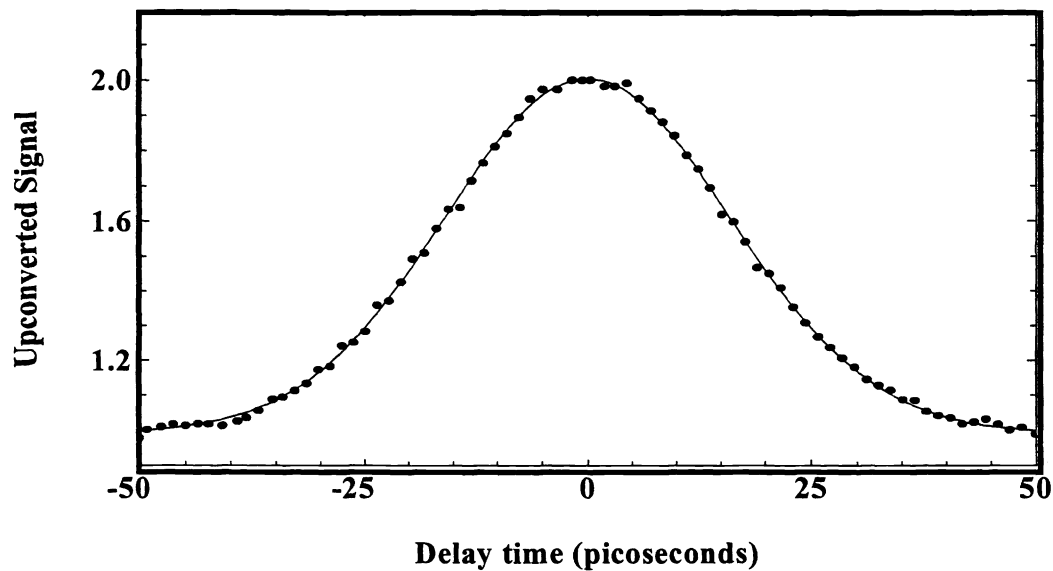


**Figure (6).** Autocorrelation of Nd:YAG laser generated in 100  $\mu\text{m}$  KD\*P crystal. The experimental data is normalised and well fitted to Gaussian function with FWHM of  $\Delta\tau = 42$  ps (the cycle points represent the experimental data and the solid line represent the calculated data).

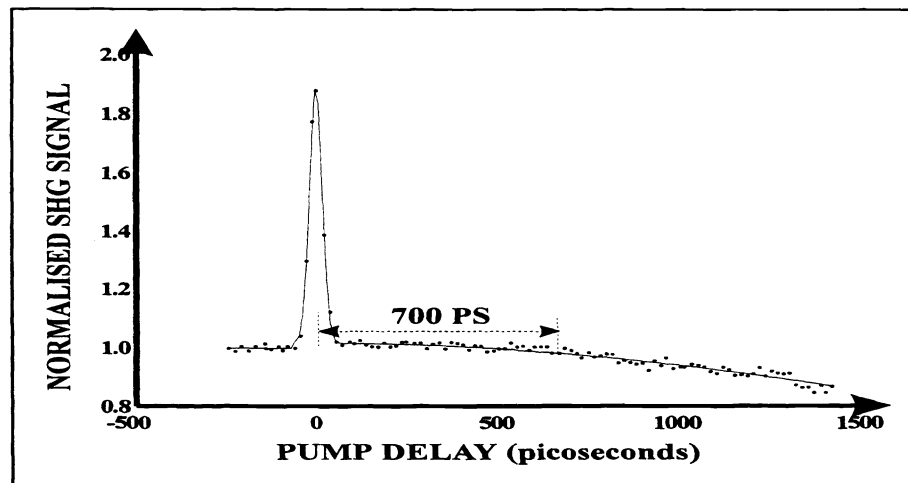


**Figure 7.** Autocorrelation of Nd:YAG laser generated in 100  $\mu\text{m}$  KD\*P crystal. The experimental data is normalized and well fitted to noise burst model of Pike and Hercher<sup>14</sup> with noise spike FWHM  $\Delta\tau = 42$ ps (the points represent the experimental data and solid line represent the calculated data).

Figure (8) shows the upconverted signal obtained for parallel and perpendicular fluorescence polarizations for a  $10^{-3}$  M solution of Rhodamine 6G in Ethanol. The signal to noise (S/N) appears to be 0.4/0.17 with a large background signal. The top graph of figure (9) shows the parallel and perpendicular fluorescence decays measured using incoherent fluorescence upconversion experiment with background removed, and the middle graph shows the log curves with background removed. The incoherent fluorescence anisotropy  $R(\tau)$  data resulting from the parallel and perpendicular polarizations data is shown in the bottom graph. It was not possible to construct an accurate  $R(\tau)$  curve from the individual decays, although from tail

matching the overall experimental  $g$ -factor was found to be  $\approx 1.18$ . The second approach of an individual analysis of the  $I_{\parallel}(\tau)$  and  $I_{\perp}(\tau)$  decays was therefore adopted using the fitting equations derived in equations (8) and (9). A direct determination of  $R(0)$ , the zero time anisotropy is not possible, however  $R(0)$  for Rhodamine 6G<sup>10</sup> is well known with experimental values slightly below the theoretical maximum of 0.4 ranging from 0.36 to 0.38. Using this range of  $R(0)$  values yields a range of reorientational times for both emission polarizations the results of which are listed in table (1) and (2). From the  $I_{\parallel}(\tau)$  data  $\tau_{or}$  was found to vary from 264 to 282 ps which compares extremely well with measurements using conventional picosecond pump-probe or fluorescence techniques<sup>2</sup>. The  $I_{\perp}$  data consistently yielded lower  $\tau_{or}$  values, ranging from 201 to 212 ps. Although these results are still in general agreement with published data for Rhodamine 6G the lower alignment contribution to the fluorescence signal would be expected to result in a less accurate value for  $\tau_{or}$ . The  $I_{\parallel}(\tau)$  and  $I_{\perp}(\tau)$  scans involve pump-gate delays out to 700 ps and on this time scale are dominated by orientational relaxation. The determination of lifetime data from these measurements would not be expected to yield accurate  $\tau_f$  values as compared to unpolarised fluorescence gating in which the contribution of the population decay to the overall signal is greater.

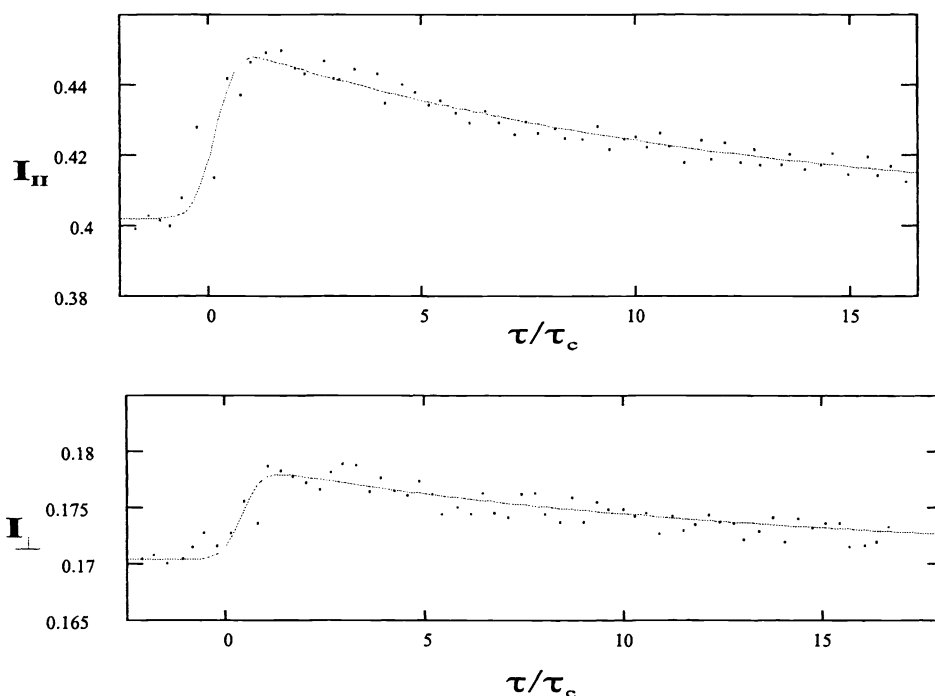


**Figure 8.** The graph shows the parallel and perpendicular fluorescence decays measured using incoherent fluorescence upconversion experiment.

## 6. CONCLUSION

In conclusion, we have presented a new method of time resolved fluorescence anisotropy measurement using incoherent laser light pulses. We have shown that the incoherent upconversion using 38 ps Gaussian noise structure of 532 nm Q-switched Nd:YAG laser pulses could be used to recover nanosecond fluorescence decays despite the presence of significant background signal. We have also shown that an individual analysis of the upconverted signals obtained for parallel and perpendicular fluorescence polarization decay for a  $10^{-3}$  M solution of Rhodamine 6G in Ethanol has been adopted using our fitting equations for  $I_{\parallel}(\tau)$  and  $I_{\perp}(\tau)$ .

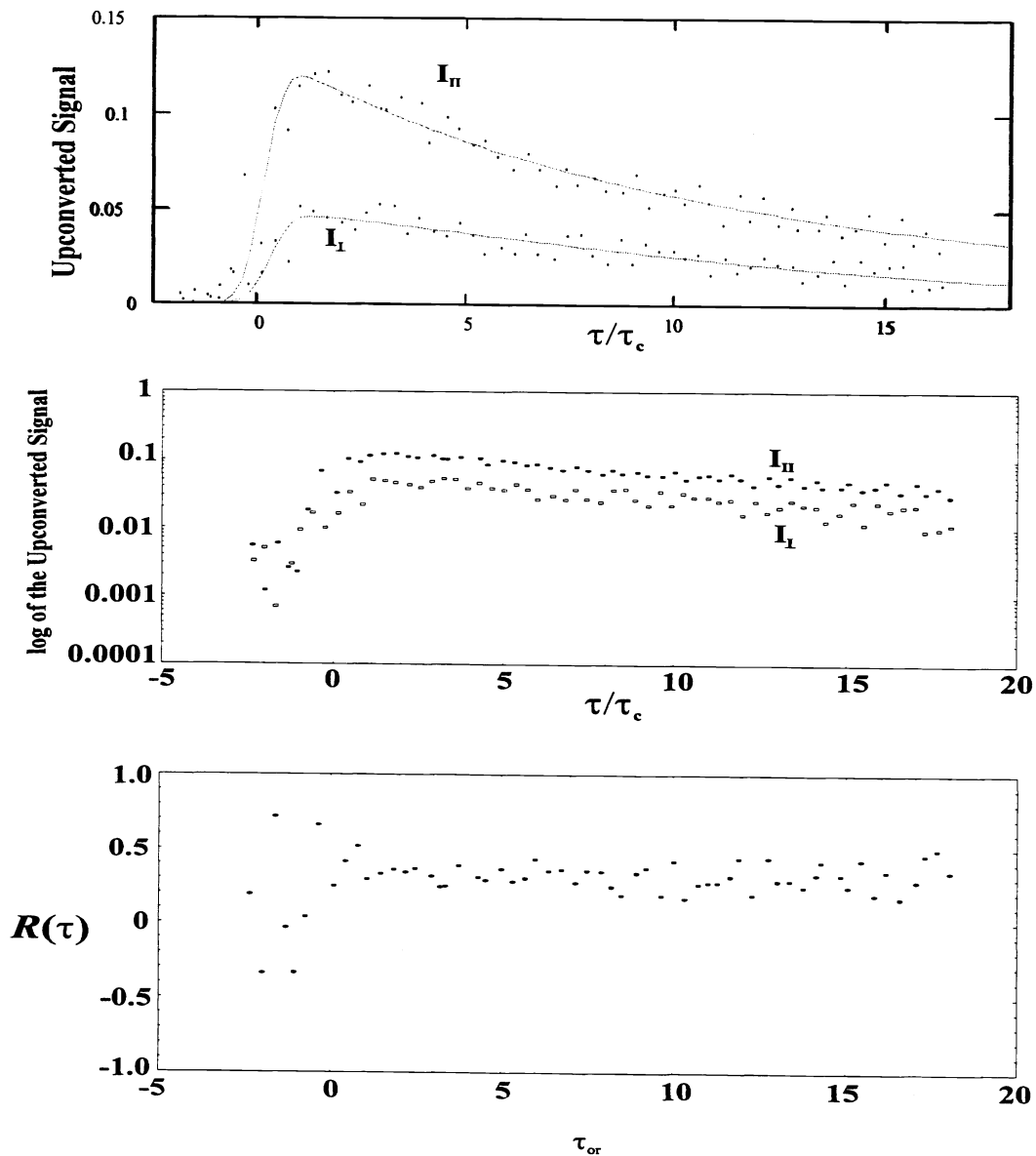


**Figure (9).** The parallel and perpendicular fluorescence decays measured using incoherent fluorescence upconversion experiment is shown in the top graph with background removed. The log curves for parallel and perpendicular are shown in the middle graph with the background removed. The incoherent fluorescence anisotropy  $R(\tau)$  data resulting from the parallel/perpendicular polarizations data is shown in the bottom graph.

<b>R(0)</b>	<b><math>\tau_{or}</math> (ps)</b>
0.36	282
0.365	276
0.37	272
0.375	265
0.38	264

**Table 1.** A range of  $\tau_{or}$  values calculated with different values of  $R(0)$  by fitting equation (8) to the  $I_H(\tau)$  data of figure (8).

<b>R (0)</b>	<b><math>\tau_{or}</math> (ps)</b>
0.36	212
0.365	206
0.37	204
0.375	203
0.38	201

**Table 2.** A range of  $\tau_{or}$  values calculated with different values of  $R(0)$  by fitting equation (9) to the data of figure (8).

## 7. ACKNOWLEDGEMENTS

We would like to thank Dr. Squire A., for his practical assistance in this work and also would like to thank King Abdulaziz City for Science and Technology (KACST), Riyadh, Saudi Arabia for their financial support.

## 8. REFERENCES

1. D. V. O'Conner and D. Phillips, "Time-Correlated Single Photon Counting", Academic Press, London, 1984.
2. G. R. Fleming, "Chemical application of Ultrafast Spectroscopy", Oxford University Press, 1986.
3. L. B. Johansson, A. Davidson, G. Lindblom and K. R. Naqvi, "Electronic Transitions in the Isoalloxazine Ring and Orientation of Flavins in Model Membranes studied by Polarised Light Spectroscopy", Biochemistry journal, Vol. 18, p.4249, 1979.
4. S. M. Arakelyan, G. A. Lyakov and Y. S. Chilingaryan, "Nonlinear Optics of Liquid Crystal", Sov. Phys. Usp., Vol. 23, 245, 1980.
5. T. P. Burghardt, , "Model Independent Fluorescence Polarization for Measuring Order in a Biological Assembly", Biopolymers, Vol. 23, p. 2384, 1984.
6. G. S. Beddard, T. Doust, and G. Porter, " Picosecond Fluorescence Depolarisation Measured by Frequency Conversion", Chemical Physics, Vol. 61, pp. 17-23,1981.
7. P. Myslinski, D. Wiczorek and K. Kownacki, "Picosecond Fluorescence Anisotropy Measured by Frequency Conversion", Chem. Phys. Lett., Vol. 155, No. 3, pp. 256-261, 1989.
8. T. Hattori and T. Kobayashi, "Ultrafast Optical Kerr Dynamics Studies With Incoherent Light" J. Chem. Phys., 94 (5), pp. 3332-3345, 1991.
9. A. A AL-Ghamdi, "Incoherent Laser Light as a Probe of Ultrafast Molecular Relaxation Dynamics", Ph.D Thesis, University of Essex, March 1996.
10. P. Chandna, "Time Resolved Fluorescence Studies of Molecular Alignment and Orientational Motion in Anisotropy Fluid Media", Ph.D Thesis, University of Essex, 1995.
11. T. Tao, "Time-Dependent Fluorescence Depolarisation and Brownian Rotational Diffusion Coefficients of Macromolecules", Biolymers., Vol. 8, pp. 609-632, 1969.
12. P. H Sarkies, "A Stable YAG Resonator Yielding a Beam of Very Low Divergence and High Output Energy", Optics Commu. Vol. 31, pp. 189-192, 1979.
13. D. C Hanna, C, G Sawyers, and M. A Yaratich, "Large Volume TEM<sub>00</sub> Mode Operation of Nd:YAG Lasers", Optics Commu., Vol. 37, pp. 359-362, 1981., and D. C Hanna, C. G Sawyers, and M. A Yaratich, "Telescope Resonators For Large-Volume TEM<sub>00</sub>-Mode Operation", Quantum Elect. Vol. 13, pp.493-507, 1981.
14. H. P Pike and M. Hercher, "Basis for Picosecond Structure in Modelocked Laser Pulses", J. Appl. Phys., Vol. 14, No. 11, pp. 4562-4565, 1970.